

Improved Project Gradient Method for Glioma Diagnosis

Soosan Francis

Abstract— Medical Image Processing is one of the most challenging and emerging topics in today's research field. Processing of Magnetic Resonance Spectroscopic Imaging (MRSI) is one of the parts in this field. In recent years, multispectral MRI has emerged as an alternative to Ultrasound (US) image modality for clear identification of tumors. In order to analyze a disease, Physicians consider MR imaging modality is the most efficient one for identification of tumors present in Brain. Therefore, analysis on MR imaging is required for efficient disease diagnosis. The nosologic images of the brain using magnetic resonance spectroscopic imaging (MRSI) data in an unsupervised way is created to differentiate various tissue patterns of glioma (Brain Tumor). Different tissue patterns are identified from the MRSI data using improved project gradient method for nonnegative matrix factorization and are then coded as different primary colors (i.e. red, green, and blue) in an RGB image, so that mixed tissue regions are automatically visualized as mixtures of primary colors. Nosologic images is useful in assisting glioma diagnosis, where several tissue patterns such as normal, tumor, and necrotic tissue can be present in the same voxel/spectrum. Error-maps based on linear least squares estimation are computed for each nosologic image to provide additional reliability information, which may help clinicians in decision making. Thus detection and extraction of brain tissue from MRI image is effectively done for glioma diagnosis

Index Terms— hierarchical nonnegative matrix factorization (hNMF), magnetic spectroscopic imaging (MRSI), nosologic imaging, non negative matrix factorization(NMF).

1 INTRODUCTION

Exact analysis of brain tumors is of one of the utmost significant work in planning, therapy, and conducting surgery. Magnetic resonance spectroscopy imaging (MRSI) is an innovative non invasive imaging technique that supplements conventional magnetic resonance imaging (MRI) by delivering multivoxel spectra of specific biochemical information associated to the tumor nature and grade. Magnetic Resonance Imaging (MRI) is an advanced medical imaging technique used to produce high quality images of the parts contained in the human body. MRI uses magnetic field and pulses of radio waves. Magnetic Resonance Spectroscopic Imaging (MRSI) provide information about the spatial metabolic heterogeneity of an organ in the body and to detect regions with abnormal tissue metabolism. The main drawback of MRI and MRSI in clinical practice is that the analysis of data requires lot of expertise from radiologist [4]. Contemporary studies have utilized MRSI or shared MRI with an MRSI to build nosologic images.[1]-[5]. The nosologic image aim at providing tumor type and grade in a single image, where different tissue forms are encoded with diverse colors. The earlier work on nosologic imaging has been based on supervised grouping procedures. The main drawback of the supervised grouping was obtaining enormous datasets for training classifiers was not always practicable. Glioma, is a type of tumor that starts in the brain or spine (glial cells). Glial cells are the tissue that supports and surrounds neurons in the brain. This are the most popular primary tumors in adults, and can be heterogeneous and infiltrative, especially for the higher grade cases. Which makes the surgical removal very impossible and complicate. MRSI may contain voxels indicating influence from various tissues, blended in random percentages.

Nosologic images where "mixed tissue" is considered as separate class[4] disregard the fact that the percentages of each tissue patterns in each "mixed" voxel may differ significantly. In general, envisioning clear contours (e.g., tumor, normal tissue, and, possibly, mixed tissue) is not practical for assorted brain tumors such as glioma. Thus, the tumoral region of glioma can consist of several tissue patterns, namely normal tissue (called 'normal'), actively growing tumor tissue (referred to as 'tumor') and necrotic tissue consisting of dead cells (referred to as 'necrosis'). Moreover, gliomas are highly infiltrative and present patterns very similar to those of other brain tumors (i.e. metastasis, lower grade). These characteristics have posed serious difficulties in the diagnosis and prognosis of glioma. The identification and localization of normal, tumor and necrosis patterns can provide added value to the clinical investigation of glioma for the guidance of therapy and determination of prognosis (i.e. the presence and amount of tumor and necrosis indicate the aggressiveness). Here the demonstration of fully Unsupervised method based on blind source separation (specifically, on nonnegative matrix factorization (NMF)[6]) to automatically create nosologic images of glioma is done and issues of image reliability is addressed by displaying "error -maps". NMF was used to differentiate brain tumor tissue from normal tissue without the need of model spectra[7]-[9]. Recent studies showed that the hierarchical tissue pattern differentiation method utilising NMF(hNMF) is able to separate three tissue patterns present in glioblastoma multiforme[10]. As an disapproval to current nosologic imaging methods[1]-[5], where one colour represents one tumor class, The unsupervised nosologic imaging summarizes the presence of different tissue and lesions in a single image by color coding each voxel or pixel according to histopathological class it's assigned to. A nosologic images provide an image guided surgery of brain tumour. Unsupervised nosologic imaging method provides mixtures of primary colors (i.e., red, green, and blue) between different tissue patterns; hence, the

● Soosan Francis is currently pursuing masters degree program in software engineering in Sri Krishna College of Engineering and Technology. Email id: suzane.francis89@gmail.com

information of mixed tissue, i.e., the information about tumor heterogeneity is maintained.

2 METHODOLOGY

2.1 Data Preprocessing

Image pre-processing is the term for operations on images at the lowest level of abstraction. The aim of the preprocessing step is to remove the irrelevant information, while enhancing the key features in order to extract them. MRS signals are affected by the presence of artifacts, instrumental errors, noise and other unwanted components. The spectral quality can be considerably improved by appropriate manipulation of the data. The sequence of preprocessing methods should be chosen carefully since one step may influence the other. These operations do not increase image information content, but they decrease it if entropy is an information measure. Pre-processing of MRI images is the primary step in image analysis which perform image enhancement and noise reduction techniques which are used to enhance the image quality, then some morphological operations are applied to detect the tumor tissue in the image. The morphological operations are basically applied on some assumptions about the size and shape of the tumor and in the end the tumor tissue are mapped onto the original gray scale image with 255 intensity to make visible the tumor in the image. The residual water removal can be performed by a subspace-based modelling approach such as HLSVD-PRO. The user can apply a HLSVDPRO filtering [LMV+02] on the following region [-499,-280] and [-32,499] Hz. Data preprocessing was done as in the previous paper [10] using the in-house software SPID. The aim of SPID is to provide the user with tools capable to simulate, preprocess, process (quantification and feature extraction) and classify in vivo and ex vivo MRS signals. These tools are embedded in a matlab graphical user interface (GUI). (Pre)processing and classification methods can be automatically run in a row using the matlab command line. The residual water components is removed using Hankel-Lanczos singular value decomposition with partial re orthogonalization (HLSVD-PRO), setting the model order to 30 and the pass band from 0.25 to 4.2 parts per million (ppm). The real parts of the preprocessed spectra were truncated to the region 0.25–4.2 ppm, resulting in $m=519$ points. To guarantee the non-negativity for NMF, the negative values were set to zero as they were caused by noise.

2.2 Tissue Differentiation

For any MRI dataset, matrix X to include spectra as column vectors, one voxel for each column. Each column of this matrix can be approximated as a linear arrangement of r fundamental spectra (i.e., "spectral sources") of specific tissue patterns [8], leading factorization.

$$\text{subject to } W, H \geq 0 \quad (1)$$

Each column of W represents a spectral source. Each row of H contains the linear order of weights. Spatial distribution information of each tissue pattern can be delivered by re-shaping each row of H back to the original spatial dimensions. The traditional NMF [6] can differentiate only two tissue patterns (i.e., normal and abnormal) by assigning the value of spectral sources r equals to 2. This is sufficient instance in the case of lower grade glioma. The common NMF is not always feasible and precise to retrieve more than two biologically meaningful spectral sources, which is most important for three tissue patterns. In such instances hierarchical NMF (hNMF) method has to be used [10]. An hNMF first separates the brain tissue into normal and abnormal, then by applying an optimized threshold, the abnormal tissue is further separated into actively proliferating tumor and necrosis. During the first level NMF is applied to the matrix of all spectra within the selected grid with the number of sources chosen to be two. Two spectral profiles and their corresponding h-maps (H_{normal} and H_{abnormal}) are recovered. The spectral sources obtained are automatically assigned to 'normal' and 'abnormal' tissue (W_{normal} and W_{abnormal}) based on the NAA/Lips (where the NAA and Lips values are estimated as the maximum intensity in the frequency regions around 2.01 and 1.3 ppm, respectively). The source with the higher NAA/Lips ratio corresponds to normal tissue and the source with the lower NAA/Lips ratio corresponds to abnormal tissue [8]. Second level NMF is performed with two sources repeatedly, on several sets of voxels, and the best result is chosen. During the third level NNLS re-estimation, the NNLS is applied to the grid considered in first level using the sources W_{normal} , W_{tumor} and W_{necrosis} to re-estimate the corresponding h-maps. In this way, the three most meaningful spectral sources for GBMs are recovered, as well as their spatial distribution information. The decision whether two or three spectral sources are more appropriate for each MRSI dataset can be based on the absence or presence of necrosis, which is a hallmark of GBM.

This can be automatically identified by specific spectral characteristics in MRSI data (i.e., integrating the region encompassing the lipid peaks at 0.9 and 1.3 ppm and comparing these values against the integrated values for the NAA at 2.01 ppm and Cho peak sat 3.22 ppm). It is important to note that spectra that are very noisy (i.e., spectra for which the peaks of interest are embedded in noise) or distorted might hinder a successful source separation by NMF. Therefore, all steps involving hNMF are typically applied on spectra of sufficient quality from smaller regions of interest (ROI) within the PRESS excitation volume. To ensure sufficient spectral quality.

$X_{m \times n} = WH$

2.3 Nosologic Imaging

With (h) NMF, the most pertinent tissue-specific spectral sources are retrieved as columns of W , as well as the three dimensional dispersal of each tissue patterns, as rows of H . Though, the spatial dispersal in H only imparts localization info about the voxels within the selected region of interest. To evaluate the involvement of each tissue pattern in the whole PRESS excitation size (thus even exterior of the chosen ROI), non negative least squares (NNLS) [14] is applied on spectra by utilizing previously recovered tissue-specific spectral sources in W . In this way the non negative least square problem is resolved for each voxel x_i .

$$\min \|x_i - Wh_i\| \text{ over } h_i \geq 0, \quad h_i \in R^r \quad (2)$$

By remodelling the set of h_i reverse into the initial matrix size. The new spatial distributions for all the r tissue patterns are acquired, each measurement representing one tissue pattern. The new spatial distribution of each tissue pattern (normalized between 0 and 1) as a color channel in an RGB image by encoding the spatial distribution for necrosis as red channel (if not present, this channel is set to zero), the one for tumor as green channel and the one for normal tissue as blue channel. The regions where the red or green color gets darker are the most aggressive regions for the respective dataset. In this way, the spatial distribution maps of different tissue patterns are incorporated into a single nosologic image where tissue-specific regions are interpreted by different colors: blue for normal, green for tumor, red for necrosis, and mixtures of these primary colors for mixed tissues, which could represent tumor infiltration. The regions of non informative signals (i.e., for which the weights corresponding to all tissue patterns are close to zero) appear in black in an RGB color scheme.

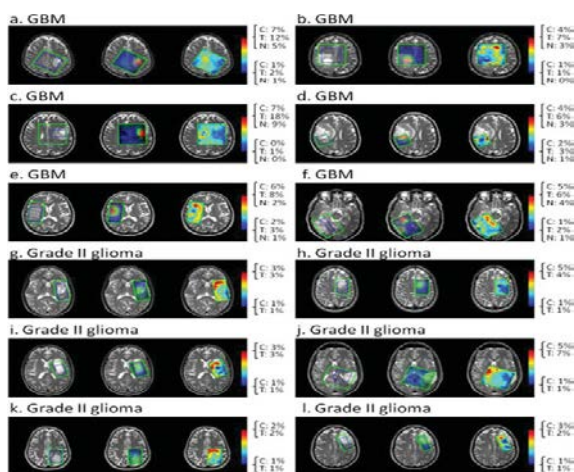


Figure 1 shows various nosologic images: First image: the anatomic T2-weighted MR image with the green box showing the

PRESS excitation volume and the blue box showing the selected region of interest (ROI). Second image: nosologic images in the PRESS excitation volume, overlaid with the anatomic MR images. The red color indicates the presence of necrosis, green shows active tumor region, and blue shows the normal region. Regions that contain noninformative signals are shown in black. Third image: the standard errors for the estimated nosologic images. On the right side of the color bars, the highest standard errors and lowest standard errors for each tissue ("C" for normal, "T" for tumor, and "N" for necrosis) are presented.

2.4 Reliability Investigation Using Standard Errors

For the least squares problems imagining that W is correctly estimated, we can approximately calculate lower bounds for the standard errors of the linear combination weights h_i at the i th voxel as the diagonal elements of the inverse information matrix $\sigma_i^2(W^T W)^{-1}$. The residual error $\|x_i - Wh_i\|$ divided by the degrees of freedom can be used to estimate σ_i^2 , which is an estimate for the noise variance for the spectrum in voxel i . The lower bounds on the standard errors for h_i at voxel i are given by

$$s_i = (\sigma_i^2 \text{diag}((w^T w)^{-1}))^{1/2} = ((\|x_i - Wh_i\|^2) / (m-r)) (\text{diag}((w^T w)^{-1}))^{1/2} \quad (3)$$

Where $m-r$ gives the statistical degree of freedom. Then standard errors are reshaped and interpolated as "error-maps" of the same size as the nosologic image, and can be interpreted as reliability maps for the nosologic image.

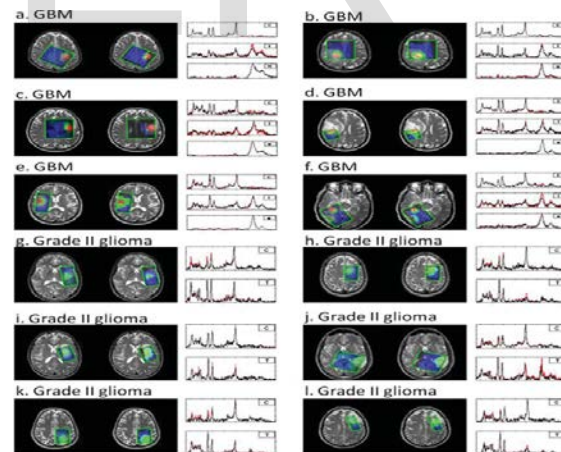


Figure 2 Showing the MR images overlaid with the nosologic images are shown in the first column. The expert labeling translated into color maps are given in the second column, where red indicates necrosis, yellow indicates necrosis/tumor, green indicates tumor, cyan indicates normal/tumor, blue indicates normal, and black indicates spectra of bad quality. In the third column, the recovered spectral sources for each tissue pattern (in black) are overlaid on the reference spectra (red). "C" stands for normal, "T" for actively proliferating tumor, and "N" for necrosis.

3 EXPECTED RESULTS

3.1 Expected Results of Nosologic Imaging

The nosologic images clearly displays the similar tissue pattern and their locations: blue for normal tissue, green for fast growing tumor, and red for necrosis. Regions of non informative spectra that are present at the outer line of PRESS excitation are displayed with black color. Mixed tissue regions are also represented using mixture of primary colors. The error maps are plotted for each nosologic image. Where red region shows the lower reliability and blue shows the higher probability.

4 CONCLUSIONS

Unsupervised nosologic imaging provides a novel way for MRSI data interpretation without the need of large training datasets. The created nosologic image is obtained on the whole PRESS excitation volume and mixed tissues in heterogeneous tumors can be shown as mixtures of primary colors. Furthermore, standard error maps provide extra information about the reliability of the nosologic images. The proposed method can also be enhanced for homogeneous tumors. Moreover, homogeneous tumors, which do not contain mixed tissues, should be easier to analyze with this approach than glioma, Since the proposed method provides a direct and effective first glance at the information contained in MRSI signals. MRSI data can be summarized in nosologic images, easily interpretable by radiologists and provide significant added value for brain tumor type diagnosis. Furthermore nosologic imaging takes into account tumor heterogeneity and can help in stereotactic biopsy guidance and therapy follow-up.

REFERENCE

[1] F. Szabo de Edelenyi, C. Rubin, F. Esteve, S. Grand, M. Decors, V Lefournier, J. F. Le Bas, and C. Remy, "A new approach for analyzing proton magnetic resonance spectroscopic images of brain tumors: Nosologic images," *Nat. Med.*, vol. 6, pp. 1287–1289, 2000.

[2] A. W. Simonetti, W. J. Melssen, M. van der Graaf, A. Heerschap, and L. M. C. Buydens, "A chemometric approach for brain tumor classification using magnetic resonance imaging and spectroscopy," *Anal. Chem.*, vol. 75, no. 20, pp. 5352–5361, 2003.

[3] T. Laudadio, M. C. Martinez-Bisbal, B. Celda, and S. Van Huffel, "Fast nosological imaging using canonical correlation analysis of brain data obtained by two-dimensional turbo spectroscopic imaging," *NMR Biomed.*, vol. 21, no. 4, pp. 311–321, 2008.

[4] M. De Vos, T. Laudadio, A. W. Simonetti, A. Heerschap, and S. Van Huffel, "Fast nosologic imaging of the brain," *J. Magn. Reson.*, vol. 184, no. 2, pp. 292–301, Jan. 2007.

[5] J. Luts, T. Laudadio, A. J. Idema, A. W. Simonetti, A. Heerschap, D. Vandermeulen, J. A. K. Suykens, and S. Van Huffel, "Nosologic imaging of the brain: segmentation and classification using MRI and MRSI," *NMR Biomed.*, vol. 22, no. 4, pp. 374–90, 2009.

[6] D. D. Lee and H. S. Seung, "Learning the parts of objects by non-negative matrix factorization," *Nature*, vol. 401, pp. 788–791, 1999.

[7] P. Sajda, S. Du, T. R. Brown, R. Stoyanova, D. C. Shungu, X. Mao, and L. C. Parra, "Nonnegative matrix factorization for rapid recovery of constituent spectra in magnetic resonance chemical shift imaging of the

brain," *IEEE Trans. Med. Imag.*, vol. 23, no. 12, pp. 1453–1465, Dec. 2004.

[8] Y. Su, S. B. Thakur, S. Karimi, S. Du, P. Sajda, W. Huang, and L. C. Parra, "Spectrum separation resolves partial-volume effect of MRSI as demonstrated on brain tumor scans," *NMR Biomed.*, vol. 21, pp. 1030–1042, 2008.

[9] S. Du, X. Mao, P. Sajda, and D. C. Shungu, "Automated tissue segmentation and blind recovery of 1 H MRS imaging spectral patterns of normal and diseased human brain," *NMR Biomed.*, vol. 21, pp. 33–41, 2008.

[10] Y. Li, D. M. Sima, S. Van Cauter, A. Croitor Sava, U. Himmelreich, Y. Pi, and S. Van Huffel, "Hierarchical non-negative matrix factorization(hNMF): A tissue pattern differentiation method for glioblastoma multiforme diagnosis using MRSI," *NMR Biomed.*, to be published.

[11] D. N. Louis, H. Ohgaki, O. D. Wiestler, W. K. Cavenee, P.C. Burger, A. Jouvret, B. W. Scheithauer, and P. Kleihues, "The 2007 WHO classification of tumors of the central nervous system," *Acta. Neuropathol.*, vol. 114, pp. 97–109, 2007.

[12] P. A. Bottomley, "Spatial localization in NMR-spectroscopy in vivo," *Ann. N. Y. Acad. Sci.*, vol. 508, pp. 333–348, 1987.

[13] J. B. Poulet, "Quantification and classification of magnetic resonance spectroscopic data for brain tumor diagnosis," Ph.D. dissertation, Dept. Elect. Eng., Katholieke Universiteit Leuven, Leuven, Belgium, 2008.

[14] C. L. Lawson and R. J. Hanson, *Solving Least-Squares Problems*. Englewood Cliffs, NJ: Prentice-Hall, 1974, ch. 23, p. 161.

[15] C. De Boor, *A Practical Guide to Splines*. New York: Springer-Verlag, 1978.